2007-01-3116

Improvement of Risk Assessment from Space Radiation Exposure for Future Space Exploration Missions

M. Y. Kim[1,2], A. L. Ponomarev[1,3], H. Nounu[1,4], H. Hussein[1,4], and F. A. Cucinotta[1]
[1]NASA Johnson Space Center
[2]Wyle Laboratories, Inc.
[3]Universities Space Research Association
[4]University of Houston

William Atwell
The Boeing Company

ABSTRACT

Protecting astronauts from space radiation exposure is an important challenge for mission design and operations for future exploration-class and long-duration missions. Crew members are exposed to sporadic solar particle events (SPEs) as well as to the continuous galactic cosmic radiation (GCR). If sufficient protection is not provided the radiation risk to crew members from SPEs could be significant. To improve exposure risk estimates and radiation protection from SPEs, detailed evaluations of radiation shielding properties are required. A model using a modern CAD tool ProE™, which is the leading engineering design platform at NASA, has been developed for this purpose. For the calculation of radiation exposure at a specific site, the cosine distribution was implemented to replicate the omnidirectional characteristic of the 4π particle flux on a surface. Previously, estimates of doses from SPEs to the blood forming organs (BFO) were made using an average body-shielding distribution for the bone marrow based on the computerized anatomical man (CAM) model. The development of an 82-point body-shielding distribution at BFOs made it possible to estimate the mean and variance of SPE doses in the major active marrow regions. Use of the detailed distribution of bone marrow sites and implementation of the cosine distribution of particle flux is shown to provide improved estimates of acute and cancer risks from SPEs.

INTRODUCTION

NASA follows radiation exposure limits (Cucinotta and Durante 2006) and implements appropriate risk mitigation measures to ensure that humans can safely live and work in the space radiation environment anywhere, anytime. In the context of the radiation protection principle of "as low as reasonably achievable" (ALARA), "safely" means that acceptable risks are not exceeded during crew members' lifetimes, where "acceptable risks" include limits on post-mission and multi-mission consequences. In design of future space missions and for the implementation of health protection measures, accurate predictions of astronauts' radiation exposure are required. In the simulation of lunar radiation interactions of large SPEs, radiation transport properties of shielding materials and astronaut's body tissues were calculated by the BRYNTRN code system (Cucinotta *et al*. 1994). In the previous work for future space mission design (Kim *et al*. 2005), a typical shield configuration was approximated as a spherical structure and one of sensitive sites of blood-forming organ (BFO) was taken as an average body-shielding distribution of the bone marrow using the computerized anatomical man (CAM) model based on the astronaut body geometry (Billings and Yucker 1973). With these approximations, the overall exposure levels at the sensitive sites were reduced to within the current exposure limits from a large SPE by adding effective polyethylene shielding to various spacecraft thicknesses.

In the development of an integrated strategy to provide astronauts maximal radiation protection with consideration of the mass constraints of space missions, the focus of the current work was to provide several considerations in detail for the improvement of risk assessment. Detailed variations of radiation shielding properties were modeled using the modern CAD tool ProE™ (2004). It represents a significant improvement in shielding analysis because it provides an analysis tool on the identical platform of most engineering designs of space vehicles. Other consideration includes the correctly aligned geometries between human and vehicle at a specific exposure site and the correction of particle source to replicate the omnidirectional characteristic of the 4π particle flux on a surface. Because the specific doses at various BFOs account for the considerable variations of proton fluences across marrow regions, an 82-point body-shielding distribution

at BFOs was developed and the mean and variance of SPE doses were calculated with the detailed distributions of major active marrow regions of head and neck, chest, abdomen, pelvis, and thighs.

The current considerations are among many requirements that must be met to improve the estimation of effective doses for radiation cancer risks. By implementing the distribution of shielding properties, detailed directional risk assessment was visualized, which can guide development of the ultimate protection for risk mitigation inside a habitable volume during future exploration missions.

APPROACH TO RISK ASSESSMENT

Space radiation is a large health concern for astronauts who are involved in space missions outside the Earth's geomagnetic field. In addition to the continuous background exposure to GCR, sporadic exposure to SPEs presents the most significant risk for short-stay (<90 d) lunar missions. The risk of early effects is very small due to the reduction of dose-rates behind shielding (<1 cGy/h) for most SPEs (Cucinotta and Durante 2006), but radiation sickness is a concern for extra-vehicular activities (EVAs) on the Moon where shielding will be at a minimum. The physical compositions and intensities of historically large SPEs are routinely examined in sensitive astronaut tissues behind various shielding materials using the Baryon transport code, BRYNTRN (Cucinotta *et al*. 1994), to predict the propagation and interactions of the deep-space nucleons through various media. The radiation risk at the sensitive tissue sites and the effective dose were assessed with the transported properties of the shielding materials and the astronauts' body tissue. The representative shield configurations for spacesuit and spacecraft were assumed to be aluminum with spherical thickness. Body-shielding distributions at sensitive organ sites of astronaut surrounding a specific point were generated using the CAM model (Billings and Yucker 1973). The point particle fluxes that traversed the tissue equivalent material of water for 512 rays were calculated at a specific anatomical area inside a shield. Assessment of radiation risk at a specific organ or tissue was calculated with the point particle fluxes. The effective dose (*E*), which is currently used for NASA operational radiation protection program, is the representative quantity of stochastic effects for the human body, where the radiation quantities of individual organs or tissues are multiplied by their respective tissue weighting factors (ICRP60, NCRP116). Figure 1 shows the exposure levels in free space as a function of the thickness of aluminum and graphite shielding in a spherical configuration for the August 1972 SPE (King 1972).

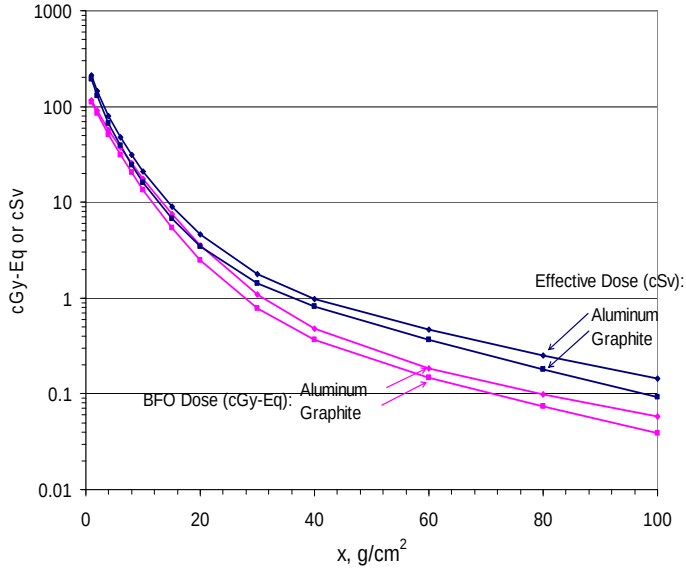

Figure 1. Effective dose and BFO dose behind aluminum and graphite shielding materials in free space from August 1972 solar particle event.

Structural design and variations of material composition layers have been considered for the total integrated shielding calculations by utilizing the CAMERA ray-tracing algorithm at several dose measurement locations for the space shuttle and the International Space Station lab module (Saganti *et al*. 2001). At each dose location, evenly spaced distributions of 512 rays over a 4π solid angle were used to calculate the point flux of a given ambient radiation. In Table 1, the exposure estimates obtained from the ray tracing are compared with the values at the average shielding thickness of each dosimetry locations (DLOCs) of the space shuttle from August 1972 SPE. The latter values are taken from the spherical configuration in the Figure 1, and the results surely show a large difference. The improved exposure estimates were made after accounting for the structural configuration by utilizing ray tracing.

Table 1. Radiation exposure levels from August 1972 SPE, estimated by ray tracing and by using the average thickness of shielding at the 6 dosimetry locations of the shuttle.

Shuttle dosimetry location	Average shielding thickness, g/cm^2	Effective dose, cSv		BFO dose at the average BFO site, cGy-Eq	
		Ray tracing	$E(\overline{X})$	Ray tracing	$B(\overline{X})$
DLOC1	26.67	36.41	2.8	24.28	1.8
DLOC2	16.46	76.05	8.0	49.62	7.0
DLOC3	19.44	72.60	4.5	47.13	3.5
DLOC4	20.01	60.11	4.4	41.77	3.4
DLOC5	21.08	73.44	3.9	48.10	3.0
DLOC6	20.92	74.09	3.9	48.96	3.0

STRUCTURAL DISTRIBUTION MODEL USING PROE™

Recognizing that polymeric materials have better shielding effectiveness with reduced mass constraint (Wilson *et al*. 1995), future exploration-class spacecraft will be composed with various high-performance polymeric composites with enhanced material properties and multi-functionalities, while the basic spacecraft construction material has been aluminum. Since the low-energy protons are attenuated rapidly with shielding, the important factors for determining the exposure levels at sensitive tissue sites are the mass distributions of the detailed structural shielding materials and the astronaut's body.

To quantify the amount of directional shielding offered by material composition layers, a structural distribution model was developed to account for detailed spacecraft geometry by using the CAD tool of ProE™ (2004). All of the structural components and contents, such as various racks, equipments, and inner and outer shell materials of the exploration-class spacecraft, were included into the model with the detailed atomic/molecular compositions, their bulk densities, and the linear dimensions for the ray-tracing calculation. Each ray evaluates the directional distribution of material intersections for space radiation propagation to a specific interior dosimetry evaluation point. Using the characteristic of shield property, which depends on the basic atomic/molecular and nuclear processes, the complexity of vector rays with actual materials is equated to the vector rays of a specified common spacecraft material, e.g. aluminum-equivalent, according to the following equation:

$$T_{Al-eq} = T_{Mat} \times \frac{R_{Al}(p_{50MeV})}{R_{Mat}(p_{50MeV})} = X_{Mat} \times \rho_{Mat} \times \frac{R_{Al}(p_{50MeV})}{R_{Mat}(p_{50MeV})} \quad (1)$$

where
$T_{Al\text{-}eq}$: Areal density of aluminum-equivalent, in g/cm^2
T_{Mat}: Areal density of a material, in g/cm^2
X_{Mat}: Linear thickness of a material, in cm
$R_{Al}(p_{50\ MeV})$: Range of 50 MeV proton beam on aluminum, in g/cm^2
$R_{Mat}(p_{50\ MeV})$: Range of 50 MeV proton beam on a target material, in g/cm^2
ρ_{Mat}: Bulk density of a material, in g/cm^3

A new fully automated method uses a complete list of actual materials for selection and allows the ray-tracings for the equivalent thickness of any given material at the user-specific dosimetry points for the evaluation of shielding. Figure 2 shows an example of the structural distribution model developed using ProE™. Figure 3a and Figure 3b show the integrated shielding thickness distributions obtained from this model at four different dosimetry locations. It clearly shows inherent directional variation of shielding thickness, which can be easily used to locate hot spots in a habitable volume.

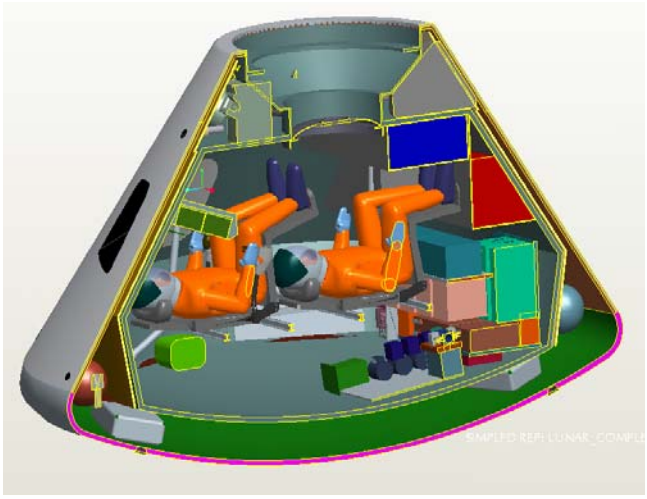

Figure 2. Structural distribution model of various composition layers for exploratory-class spacecraft developed using ProE™

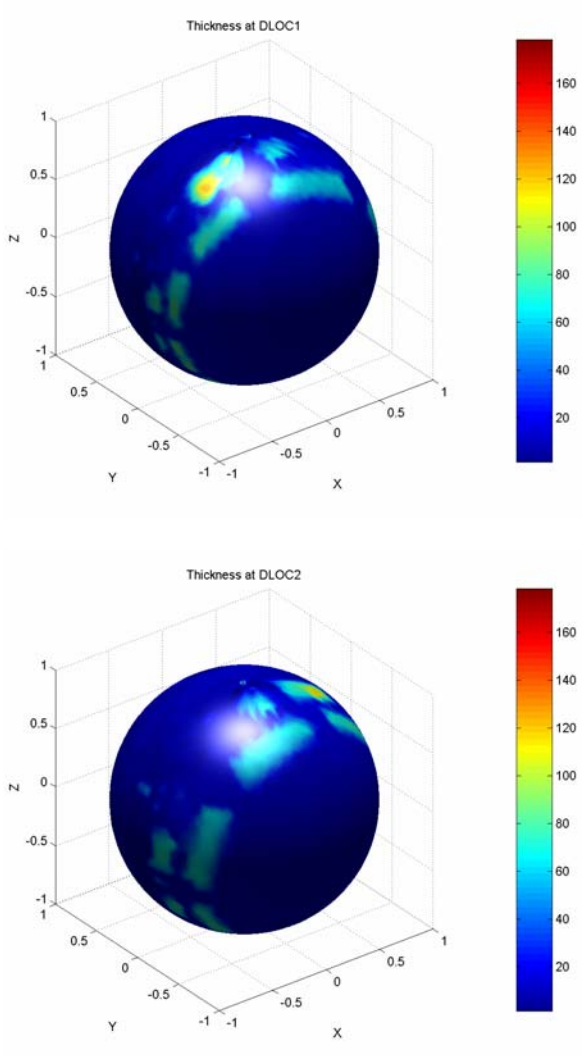

Figure 3a. Shielding distributions at 2 locations inside a spacecraft: DLOC1 and DLOC2.

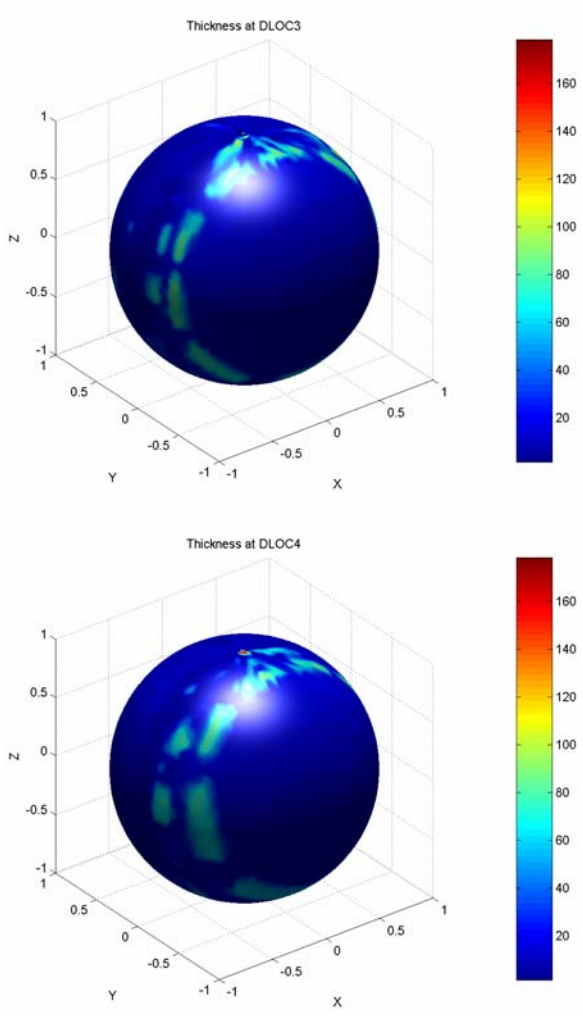

Figure 3b. Shielding distributions at the other 2 locations inside a spacecraft: DLOC3 and DLOC4.

RADIATION SOURCE CONSIDERATION

For the principal goal of planetary radiation simulation at a critical site of human body inside a spacecraft, habitat, or spacesuit during EVA on the lunar or Mars surface, the production of emitted ion spectra including nuclear secondaries was predicted by solving the fundamental Boltzmann transport equation for the propagation and interaction of the deep-space nucleons and heavy ions through various media. The fully coupled all-energy, all-particle simulation was made for a given number of rays by using the new fully automated ray-tracing model, in which detailed radiation shielding properties were fully accounted for each ray with each separate medium's thickness distribution along a ray surrounding at a specific position. Similarly, radiation point flux at a specific organ site was calculated with detailed body-shielding properties at the site of human body geometry using the CAM model based on the 50 percentile United States Air Force male in the standing position (Billings and Yucker, 1973). The shielding distribution can be treated as being randomly oriented for spacecraft and body organs or as being in a fixed alignment when evaluating organ doses inside spacecraft. Either case is an idealization of the actual motion of an astronaut inside a spacecraft or habitat.

For the randomly oriented calculation with discrete number of scattered rays, the angular description of incident particle on a specific location is treated as an isotropic angular distribution:

$$p(\mu) = \text{constant} \qquad (2)$$

where μ is the cosine of the angle between the particle direction (the ray) and the surface normal (on the surface of a specific organ site). In this way, all the incident particles are correctly treated as the normal to the specific organ site, because they are evenly scattered for the given number of rays over a 4π solid angle. The organ dose equivalent estimate, H_{organ}, is an average of the directional values for the evenly distributed number of rays with the angular particle fluxes at the organ site:

$$H_{organ} = \frac{1}{N}\sum_{i=1}^{N} H(X_i) \qquad (3)$$

where
N: the given number of rays
X_i: a shielding amount by material composition layers at i^{th} ray.

The fully coupled shielding properties between the integrated shielding by spacecraft and the body-shielding at a sequence of regularly spaced intervals of angular distributions were correctly obtained only after their orientations were correctly aligned at a specific organ site. To couple a newly developed NASA-JSC ray tracer with CAM, a smooth bivariate interpolation scheme, which is a quintic polynomial in two variables (polar and azimuth angles), was implemented for the scattered data of spacecraft and CAM. For the angular description of incident particle on a specific location with the fixed alignment, it is not an isotropic angular distribution for the continuous intervals on spherical polar coordinates. The appropriate method for describing a surface source of particles incident on a specific organ site is actually a cosine distribution:

$$p(\mu) = \mu \qquad (4)$$

for a continuously distributed source of particles at the site. In this way, the energy deposited into a volume element of an organ is correctly accounted for all the incident particles, which are regularly spaced in a small interval on spherical polar coordinates. The improved organ dose assessment at a specific anatomical location is evaluated with the correct point particle fluxes and the correctly coupled shielding thickness at each interval:

$$H_{organ} = \int_{\theta=\frac{-\pi}{2}}^{\frac{\pi}{2}} \cos\theta \, d\theta \, d\phi \, H\big(X(\theta,\phi) + Y(\theta,\phi)\big) \qquad (5)$$

where
θ: polar angle of a ray
ϕ: azimuth angle of a ray
$X(\theta,\phi)$: the integrated shielding thickness by spacecraft of a ray
$Y(\theta,\phi)$: the body-shielding thickness of a ray

CONSIDERATION OF ACTIVE BONE MARROW DISTRIBUTIONS

The most critical organ site considered for radiation protection is BFO. It has been assumed as an average body-shielding distribution for the bone marrow based on CAM model. However, quantitative estimates of the active bone marrow in adults are quite distributed over several body regions as shown in Table 2 (Cristy, 1981). Therefore, 82 specific BFO sites representing the different active regions (Figure 4) were accounted for the human body geometry using the CAM model (Atwell, 1994). Estimates of the specific dose from an SPE at each of these BFO sites inside a typical equipment room of a spacecraft (an aluminum sphere of 5 g/cm^2 thickness) on the lunar surface showed large variations (Figure 5). The considerable variance of doses across marrow sites was caused by the characteristic spectra of proton fluence at each site, and it made the use of an average BFO questionable. The variations will increase further when the complexities of spacecraft shielding distributions will be accounted, which is necessary for the accurate radiation risk assessment and the protection guidelines from complex radiation fields and shielding distributions. The development of the 82-point BFO shielding distribution made it possible to estimate the mean and variance of SPE doses in the major active marrow regions of head and neck, chest, abdomen, pelvis, and thighs (Figure 6). It will also allow more accurate estimates of the marrow response to estimate the radiation risk of leukemia, which could be the dominant risk to astronauts from a major SPE (Cucinotta *et al*. 2006).

Table 2. Active marrow distributions in adults (age 40) calculated from anatomical data (Cristy, 1981)

Body region	Marrow distribution
Head and neck	12.2%
Chest (upper torso)	26.1%
Abdomen (mid torso)	24.9%
Pelvis (lower torso)	33.4%
Thighs (upper legs)	3.4%
Lower legs	n/a
Arms	n/a

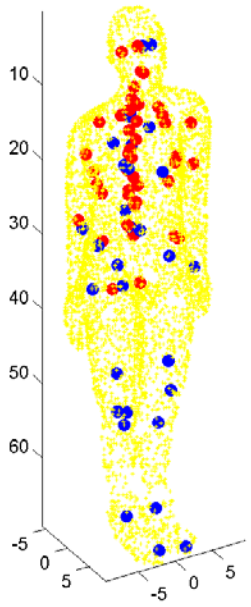

Figure 4. The 82-point BFO sites to cover the different active marrow regions.

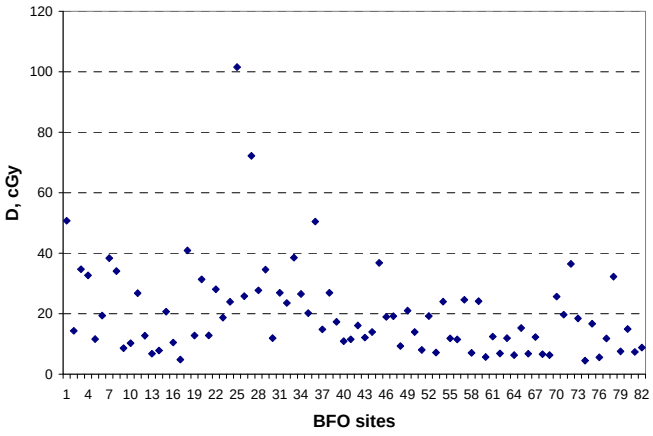

Figure 5. Absorbed dose distributions at 82 BFO sites of astronaut inside a typical equipment room of spacecraft on lunar surface from August 1972 SPE.

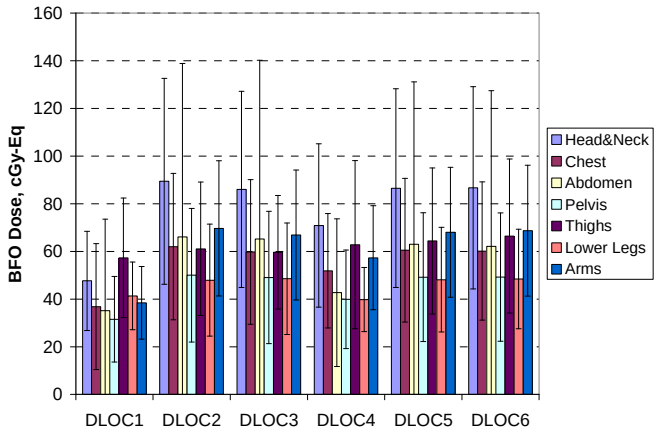

Figure 6. The average BFO doses and their standard deviations from August 1972 SPE for various body regions of active marrow sites at 6 dosimetry locations (DLOCs) of space shuttle.

RESULTS AND DISCUSSION

In the effort to make accurate assessments of radiation doses to astronauts, which are required for planning of future exploration-class and long-duration space missions (Cucinotta and Durante 2006), a fully automated structural distribution model has been developed using a CAD tool of ProE™. Visual presentation of shielding thickness clearly shows that the hot spots exist for sensitive sites of tissue/organ inside a future spacecraft, even though its overall configuration provides enough shielding from an SPE as shown in Figure 3. With the directional shielding amounts, the results of organ dose quantities for random orientation are shown in Table 3a at four different locations inside a spacecraft. We also implemented radiation source corrections for the fixed orientation: (1) correct alignment of spacecraft and body for the coupled shielding properties for each rays (2) cosine distribution for the angular description of incident particle at the sequence of regularly spaced intervals. The results are shown in the Table 3b.

Finally, detailed directional risk assessment is visualized in Figure 7 at a dosimetry location (DLOC1) inside a spacecraft. In the Figure 7a, the spacecraft is shown in a translucent view to reveal the exact dosimetry location inside a spacecraft, and the same directional dose assessment is separately shown in large view in the Figure 7b. This kind of visualization can guide the ultimate protection for risk mitigation inside a habitable volume during future exploration missions. It is evident that the top hatch or possibly a heat-shield for re-entry of a spacecraft can provide the greatest shielding effect from SPE, while areas such as windows provide the least effect. This rationale will aid development of many objective-oriented strategies, such as local shielding approaches, optimization of equipments/components as shields, and optimization of astronaut orientation.

Table 3a. Organ dose quantities of random orientation from August 1972 SPE.

		DLOC1	DLOC2	DLOC3	DLOC4
X-coordinate, cm Y-coordinate, cm Z-coordinate, cm		43.18 119.38 52.71	-43.18 119.38 52.71	40.64 119.38 -79.34	-40.64 119.38 -79.34
Al-Eq x_{avg}, g/cm^2		15.18	15.08	15.85	15.33
x_{min} x_{max}		0 102.07	0 105.50	0 83.21	0 85.79
CAM organ dose, cSv	Avg skin	126.61	121.07	104.08	108.59
	Eye	86.76	84.36	73.58	77.06
	Avg BFO	16.91	16.82	15.2	15.88
	Stomach	7.38	7.37	6.77	7.03
	Colon	14.42	14.36	13.04	13.6
	Liver	10.37	10.33	9.41	9.8
	Lung	12.16	12.12	11.04	11.5
	Esophagus	11.61	11.57	10.54	10.98
	Bladder	7.54	7.53	6.9	7.17
	Thyroid	18.39	18.31	16.55	17.28
	Chest	72.23	70.58	61.85	64.83
	Gonads	35.27	34.74	30.76	32.24
	Front brain	29.54	29.32	26.31	27.53
	Mid brain	16.2	16.15	14.68	15.3
	Rear brain	28.93	28.72	25.79	26.98
Point dose eq, cSv		254.68	242.74	207.92	216.83

Table 3b. Organ dose quantities of aligned orientation from August 1972 SPE.

		DLOC1	DLOC2	DLOC3	DLOC4
X-coordinate, cm Y-coordinate, cm Z-coordinate, cm		43.18 119.38 52.71	-43.18 119.38 52.71	40.64 119.38 -79.38	-40.64 119.38 -79.38
Al-Eq x_{avg}, g/cm^2		15.18	15.08	15.85	15.33
x_{min} x_{max}		0 102.07	0 105.50	0 83.21	0 85.79
CAM organ dose, cSv	Avg skin	150.92	135.41	111.45	114.45
	Eye	89.71	89.94	81.62	79.72
	Avg BFO	18.14	18.20	16.05	15.98
	Stomach	6.94	6.89	6.59	6.63
	Colon	14.46	14.36	12.67	12.79
	Liver	9.43	9.60	8.92	9.23
	Lung	12.09	11.61	11.30	10.73
	Esophagus	11.25	10.78	10.52	9.93
	Bladder	7.64	7.25	6.98	6.84
	Thyroid	18.55	18.15	16.47	16.79
	Chest	74.88	73.95	67.60	66.37
	Gonads	37.72	32.64	31.19	27.74
	Front brain	28.72	27.60	25.32	25.32
	Mid brain	15.52	15.56	14.05	15.03
	Rear brain	27.49	27.96	24.98	27.84
Point dose eq, cSv		253.48	241.76	205.76	211.88

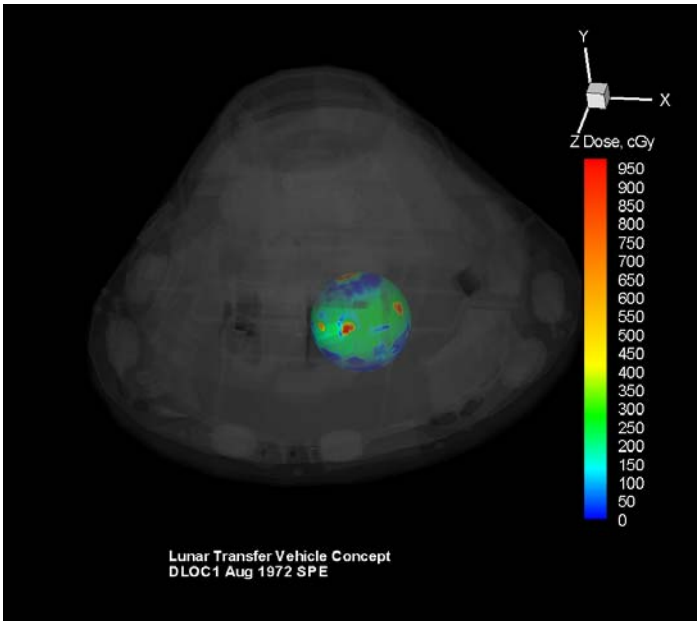

(a)

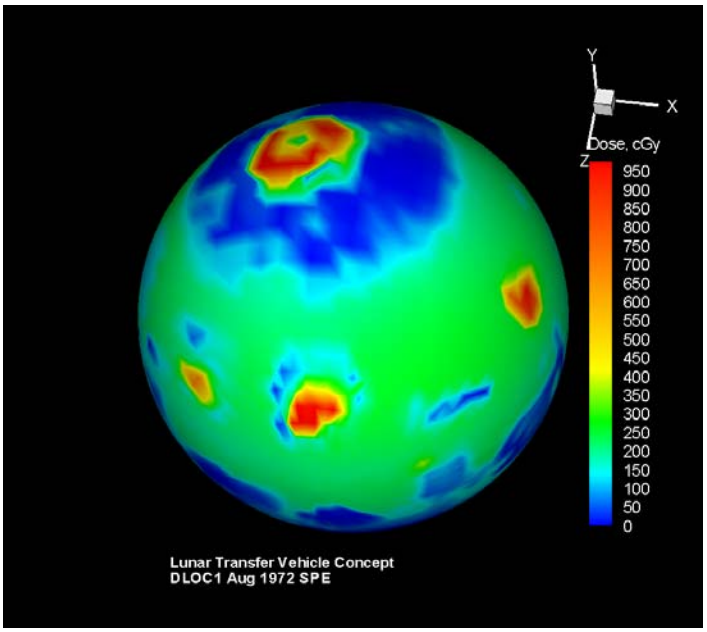

(b)

Figure 7. Visualization of detailed directional dose assessment at a dosimetry location (DLOC1) inside a space craft. (a) The spacecraft is shown in a translucent view to reveal the exact dosimetry location. (b) The directional dose assessment is shown in large view.

Because of the characteristic spectra of primary solar protons of SPEs, proton fluences and doses vary considerably across marrow regions. Detailed body-shielding distribution of 82 bone marrow sites were accounted for the active marrow regions, which faithfully reproduced the mean and the standard deviations of SPE doses in those regions. More accurate estimates of the marrow response will be used to estimate the radiation risk of leukemia from a major SPE (Cucinotta *et al*. 2006). The large variation in marrow doses has opposite results when considering acute risks versus the risk of leukemia. In considering the acute risk to the BFOs, the marrow with lower dose components is fully capable of replenishing the entire blood system. Therefore, knowledge of the variation is extremely important. For leukemia risk, a linear-quadratic dose response is found with the quadratic term being dominant at high dose (> 1 Gy) (NCRP 132). Therefore, the marrow regions with high doses are the concern since leukemia risk from a large SPE condition may contain contributions from the quadratic component of the dose-response.

In the current work, we made significant improvement of risk assessment with several considerations. Many other requirements must be improved as future work for the risk assessment and protection of astronauts, which may include new definition of age and gender related tissue weighting factors, modified transport codes with improved definitions of neutrons produced inside spacecraft, improved space environmental projection models for mission planning, and using detailed transport properties for the atomic properties of structural components, perhaps using parallel processing methods.

REFERENCES

1. Atwell, W., "Anatomical Models For Space Radiation Applications: An Overview," *Adv. Space Res.*, **14(10)**, 415-422, 1994.
2. Billings, M.P., Yucker, W.R., "The Computerized Anatomical Man (CAM) Model," NASA CR-134043, 1973.
3. Cristy, M., "Active Bone Marrow Distribution As A Function Of Age In Humans," *Phys. Med. Biol.*, **26(3)**, 389-400, 1981.
4. Cucinotta, F. A., Wilson, J. W., Badavi, F. F., "Extension To The BRYNTRN Code To Monoenergetic Light Ion Beams," NASA TP-3472, 1994.
5. Cucinotta, F.A., Durante, M., "Cancer Risk From Exposure To Galactic Cosmic Rays: Implications For Space Exploration By Human Beings," *Lancet Oncology*, **7**, 431-435, 2006.
6. Cucinotta, F. A., W. Atwell, Kim, M. Y., George, K. A., Ponomarev, A., Nikjoo, H., and Wilson, J. W., "Prediction Of Leukemia Risk To Astronauts From Solar Particle Events," 4th International workshop on space radiation research, June 5-9, 2006, Moscow, Russia.
7. International Commission on Radiobiological Protection (ICRP), 1990 Recommendations Of The International Commission On Radiobiological Protection, ICRP Publication 60, Annals of the ICRP 21, Elsevier Science, New York, 1991.
8. Kim, M.Y., Hu, X., Cucinotta, F.A., "Effect Of Shielding Materials From SPEs On The Lunar And Mars Surface," AIAA 2005-6653, 2005.

9. King, J. H., August 1972 SPE spectra, unpublished records of a NASA workshop, correspondence dated October 24, 1972, from J. H. King (NASA Goddard Space Flight Center) to A. C. Hardy (NASA Johnson Space Center).
10. National Council on Radiation Protection and Measurements (NCRP), Limitation Of Exposure To Ionizing Radiation, NCRP Report No. 116, Bethesda, MD, 1993.
11. National Council on Radiation Protection and Measurements (NCRP), Radiation Protection Guidance For Activities In Low-Earth Orbit, NCRP Report No. 132, Bethesda, MD, 2000.
12. Pro/ENGINEER® Wildfire 2.0, Parametric Technology Corporation, March 2004.
13. Saganti, P. B., Zapp, E. N., Wilson, J. W., Cucinotta, F. A., "Visual Assessment Of The Radiation Distribution In The ISS Lab Module," *Physica Medica*, **XVII (S1)**, 106-112, 2001.
14. Wilson, J.W., Kim, M., Schimmerling, W., Badavi, F.F., Thibeault, S.A., Cucinotta, F.A., Shinn, J.L., and Kiefer, R., "Issues In Space Radiation Protection," *Health Physics*, **68**, 50-58, 1995.